BULLETIN OF THE POLISH ACADEMY OF SCIENCES
TECHNICAL SCIENCES, Vol. 69(6), 2021, Article number: e138240
DOI: 10.24425/bpasts.2021.138240

The implicit numerical method for the one-dimensional anomalous subdiffusion equation with a nonlinear source term

Marek BŁASIK*

Institute of Mathematics, Czestochowa University of Technology, al. Armii Krajowej 21, 42-201 Czestochowa, Poland

Abstract. In the paper, the numerical method of solving the one-dimensional subdiffusion equation with the source term is presented. In the approach used, the key role is played by transforming of the partial differential equation into an equivalent integro-differential equation. As a result of the discretization of the integro-differential equation obtained an implicit numerical scheme which is the generalized Crank-Nicolson method. The implicit numerical schemes based on the finite difference method, such as the Carnk-Nicolson method or the Laasonen method, as a rule are unconditionally stable, which is their undoubted advantage. The discretization of the integro-differential equation is performed in two stages. First, the left-sided Riemann-Liouville integrals are approximated in such a way that the integrands are linear functions between successive grid nodes with respect to the time variable. This allows us to find the discrete values of the integral kernel of the left-sided Riemann-Liouville integral and assign them to the appropriate nodes. In the second step, second order derivative with respect to the spatial variable is approximated by the difference quotient. The obtained numerical scheme is verified on three examples for which closed analytical solutions are known.

Key words: fractional derivatives and integrals; integro-differential equations; numerical methods; finite difference methods.

1. INTRODUCTION

Diffusion is the process of spreading molecules of one substance into another. It occurs due to a phenomenon known as Brownian motion, i.e., the chaotic movement of molecules in liquids and gases, which is caused by the collision of solute molecules with the components of the fluid. It was first noticed by botanist Robert Brown while observing pollen suspended in liquids. In classical diffusion, the movement of molecules is governed by law:

$$\langle x^2(t)\rangle \sim Dt, \tag{1}$$

where $\langle x^2(t)\rangle$ is a mean squared displacement of the diffusing molecule in the course of time t, and D is the diffusion coefficient.

However, the relation (1) does not allow us to describe many transport processes that occur in nature. In the papers [1, 2] Kosztołowicz *et al.* experimentally proved that the transport of glucose and sucrose in a gel solvent is subdiffusive.

Another experimental example of anomalous diffusion is the experiment carried out by Weeks, Solomon and Swinney, the results of which are presented in the papers [3, 4], where the researchers studied the flow of fluid in a rotating ring-shaped vessel.

In the paper [5], Humphries *et al.* shows that some open-ocean predators may use Lévy flights to maximize the chances of finding prey in food-poor habitats. At the same time, this suggest that it is possible to change the foraging pattern to Brownian motion when the prey is abundant.

Differential operators of fractional order are also used in modeling problems related to thermal conduction [6].

The cited examples confirm that Brownian motion is only a special case of transport processes called anomalous diffusion, which is governed by the following law [7, 8]:

$$\langle x^2(t)\rangle \sim D_\alpha t^\alpha, \quad 0 < \alpha \leq 1, \tag{2}$$

where D_α is the generalized diffusion coefficient.

In the paper the one-dimensional subdiffusion equation with the source term is considered. In problems related to heat transfer the source term is interpreted as an internal heat source, while in the processes related to mass transfer it is related to the reaction-diffusion equation. The aim of the article is to develop a numerical method for solving the above-mentioned equation. The problem considered is governed by subdiffusion equation with time derivative in the Caputo sense. It should be noted here that most of the problems of this type considered in the literature are formulated using the Riemann-Liouville derivative [9–11].

The paper is organized as follows. In the next section, the necessary definitions and properties used in the rest of the paper are introduced. The initial-boundary value problem (IBVP) is formulated in section three for which a numerical method

*e-mail: marek.blasik@im.pcz.pl

Manuscript submitted 2021-02-25, revised 2021-05-25, initially accepted for publication 2021-06-23, published in December 2021

is developed. The fourth section contains three examples comparing the numerical results obtained by the proposed method with the closed analytical solutions. The last section contains conclusions.

2. PRELIMINARIES

At the beginning, let us define two fractional operators [12]: the left-sided Riemann-Liouville integral and the left-sided Caputo derivative and property playing an important role in further considerations.

Definition 1. The left-sided Riemann-Liouville integral of order α, denoted as I^{α}_{0+}, is given by the following formula for $\mathrm{Re}(\alpha) \in (0,1]$:

$$I^{\alpha}_{0+} f(t) := \frac{1}{\Gamma(\alpha)} \int_0^t \frac{f(\tau)\,\mathrm{d}\tau}{(t-\tau)^{1-\alpha}}, \tag{3}$$

where Γ is the Euler gamma function.

Definition 2. Let $\mathrm{Re}(\alpha) \in (0,1]$. The left-sided Caputo derivative of order α is given by the formula:

$${}^{C}D^{\alpha}_{0+} f(t) := \begin{cases} \dfrac{1}{\Gamma(1-\alpha)} \displaystyle\int_0^t \frac{f'(\tau)\,\mathrm{d}\tau}{(t-\tau)^{\alpha}}, & 0 < \alpha < 1, \\ \dfrac{\mathrm{d}f(t)}{\mathrm{d}t}, & \alpha = 1. \end{cases} \tag{4}$$

Property 1. Let function $f \in C^1(0,T)$. Then, the composition rule for the left-sided Riemann-Liouville integral and the left-sided Caputo derivative is given as follows:

$$I^{\alpha}_{0+}\,{}^{C}D^{\alpha}_{0+} f(t) = f(t) - f(0). \tag{5}$$

The next two definitions [13–16] contribute to the formation of the examples considered in section four.

Definition 3. The generalized hypergeometric function denoted as ${}_pF_q(\beta_1,\ldots,\beta_p;\gamma_1,\ldots,\gamma_q;\cdot)$ is defined by the following formula:

$${}_pF_q(\beta_1,\ldots,\beta_p;\gamma_1,\ldots,\gamma_q;z) := \sum_{k=0}^{\infty} \frac{(\beta_1)_k \ldots (\beta_p)_k}{(\gamma_1)_k \ldots (\gamma_p)_k} \frac{z^k}{k!}, \tag{6}$$

where $(\cdot)_k$ is denoting the rising factorial or Pochhammer symbol defined in terms of the Euler gamma function Γ for any real x except the non-positive integers by

$$(x)_k = \frac{\Gamma(x+k)}{\Gamma(x)}. \tag{7}$$

Definition 4. The regularized generalized hypergeometric function denoted as ${}_p\tilde{F}_q(\beta_1,\ldots,\beta_p;\gamma_1,\ldots,\gamma_q;\cdot)$ is defined by the following formula:

$${}_p\tilde{F}_q(\beta_1,\ldots,\beta_p;\gamma_1,\ldots,\gamma_q;z) := \frac{{}_pF_q(\beta_1,\ldots,\beta_p;\gamma_1,\ldots,\gamma_q;z)}{\Gamma(\gamma_1)\ldots\Gamma(\gamma_q)}. \tag{8}$$

The numerical scheme proposed in the third section of the paper uses a mesh of nodes defined as follows:

Definition 5. Let $\Pi = \{(x,t)\colon x \in [0,L];\, t \in [0,T]\}$ be a continuous region of solutions for the partial differential equation. Then the set $\overline{\Pi} = \left\{(x_i,t_j) \in \Pi\colon x_i = i\Delta x,\ i \in \{0,1,\ldots,m\},\ \Delta x = \frac{L}{m}; t_j = j\Delta t,\ j \in \{0,1,\ldots,n\};\ \Delta t = \frac{T}{n}\right\}$ we call the rectangular regular mesh described by the set of nodes.

3. MATHEMATICAL FORMULATION AND NUMERICAL SOLUTION OF THE PROBLEM

Consider the following subdiffusion equation with a nonlinear source term

$${}^{C}D^{\alpha}_{0+,t} U(x,t) = D_{\alpha} \frac{\partial^2 U(x,t)}{\partial x^2} + Q_{\alpha}(x,t), \quad 0 \le x \le L, \quad 0 \le t \le T, \tag{9}$$

supplemented with the boundary conditions

$$U(0,t) = f(t), \quad U(L,t) = g(t), \quad 0 \le t \le T, \tag{10}$$

and initial condition

$$U(x,0) = h(x), \quad 0 \le x \le L, \tag{11}$$

where the generalized diffusion coefficient D_{α} is constant.

In the paper [17] the concept of the Crank-Nicolson method for the parabolic equation was extended to the case of the one-dimensional subdiffusion equation with the time derivative in the Caputo sense. A similar approach can be applied to the initial-boundary value problem defined by equations (9)–(11), where the source term is presented.

By applying the left-sided Riemann-Liouville integral of order $\alpha \in (0,1]$ to both sides of equation (9) and using property 1 we get the integro-differential equation in the following form:

$$U(x,t) = U(x,0) + \frac{D_{\alpha}}{\Gamma(\alpha)} \int_0^t \frac{1}{(t-\tau)^{1-\alpha}} \frac{\partial^2 U(x,\tau)}{\partial x^2}\,\mathrm{d}\tau + \frac{1}{\Gamma(\alpha)} \int_0^t \frac{Q_{\alpha}(x,\tau)\,\mathrm{d}\tau}{(t-\tau)^{1-\alpha}}. \tag{12}$$

The discretization of equation (12) on the grid of nodes defined by definition 5 requires approximation of integral and differential operators. Let's start with determining the discrete values of the integral kernel of the left-sided Riemann-Liouville integrals on the right-hand side of equation (12). For this purpose, the integrant U is approximated with a linear function $\overline{U}$ between two subsequent grid nodes with respect to the time variable:

$$\overline{U}(x,t) = U(x,t_j) \frac{t - t_{j+1}}{t_j - t_{j+1}} + U(x,t_{j+1}) \frac{t - t_j}{t_{j+1} - t_j}, \tag{13}$$

for $t_j \le t \le t_{j+1}$, $j = 0,\ldots,n-1$. We act in the same way with the source term Q:

$$\overline{Q}_\alpha(x,t) = Q_\alpha(x,t_j)\frac{t-t_{j+1}}{t_j-t_{j+1}} + Q_\alpha(x,t_{j+1})\frac{t-t_j}{t_{j+1}-t_j}, \quad (14)$$

for $t_j \le t \le t_{j+1}$, $j = 0,\ldots,n-1$. It should be emphasized here that the above approximation in relation to partial differential equations of fractional order was used in [18, 19]. The author, a few years after the publication of the cited results, came to the conclusion that the discretization of the integro-differential equation in the node $(i\Delta x, k\Delta t)$ is more transparent. The previously used notation was directly inspired by the results obtained by Diethelm for the Adams-Bashforth-Moulton method in [20]. Thus, the first integral term of equation (12) on the interval $[0, t_k]$ can be approximated by the formula:

$$\frac{D_\alpha}{\Gamma(\alpha)}\int_0^{t_k}\frac{1}{(t_k-\tau)^{1-\alpha}}\frac{\partial^2 U(x,\tau)}{\partial x^2}\,\mathrm{d}\tau \approx \frac{D_\alpha}{\Gamma(\alpha)}\int_0^{t_k}\frac{1}{(t_k-\tau)^{1-\alpha}}\frac{\partial^2 \overline{U}(x,\tau)}{\partial x^2}\,\mathrm{d}\tau. \quad (15)$$

From the theorem on additivity of an integral with respect to the integration interval, we get:

$$\begin{aligned}
&\frac{D_\alpha}{\Gamma(\alpha)}\int_0^{t_k}\frac{1}{(t_k-\tau)^{1-\alpha}}\frac{\partial^2 \overline{U}(x,\tau)}{\partial x^2}\,\mathrm{d}\tau \\
&= \frac{D_\alpha}{\Gamma(\alpha)}\sum_{j=0}^{k-1}\int_{t_j}^{t_{j+1}}\frac{1}{(t_k-\tau)^{1-\alpha}} \\
&\quad\times\left(\frac{\partial^2 U(x,t_j)}{\partial x^2}\frac{\tau-t_{j+1}}{t_j-t_{j+1}} + \frac{\partial^2 U(x,t_{j+1})}{\partial x^2}\frac{\tau-t_j}{t_{j+1}-t_j}\right)\mathrm{d}\tau \\
&= \frac{D_\alpha}{\Gamma(\alpha)}\frac{\partial^2 U(x,t_0)}{\partial x^2}\int_0^{t_1}\frac{1}{(t_k-\tau)^{1-\alpha}}\frac{\tau-t_1}{t_0-t_1}\,\mathrm{d}\tau \\
&\quad+\frac{D_\alpha}{\Gamma(\alpha)}\sum_{j=1}^{k-1}\frac{\partial^2 U(x,t_j)}{\partial x^2}\left(\int_{t_{j-1}}^{t_j}\frac{1}{(t_k-\tau)^{1-\alpha}}\frac{\tau-t_{j-1}}{t_j-t_{j-1}}d\tau\right. \\
&\quad\left.+\int_{t_j}^{t_{j+1}}\frac{1}{(t_k-\tau)^{1-\alpha}}\frac{\tau-t_{j+1}}{t_j-t_{j+1}}d\tau\right) \\
&\quad+\frac{D_\alpha}{\Gamma(\alpha)}\frac{\partial^2 U(x,t_k)}{\partial x^2}\int_{t_{k-1}}^{t_k}\frac{1}{(t_k-\tau)^{1-\alpha}}\frac{\tau-t_{k-1}}{t_k-t_{k-1}}\,\mathrm{d}\tau.
\end{aligned}$$

Repeating the above reasoning for the second integral term in equation (12), we get:

$$\frac{1}{\Gamma(\alpha)}\int_0^{t_k}\frac{Q_\alpha(x,\tau)\,\mathrm{d}\tau}{(t_k-\tau)^{1-\alpha}} \approx \frac{1}{\Gamma(\alpha)}\int_0^{t_k}\frac{\overline{Q}_\alpha(x,\tau)\,\mathrm{d}\tau}{(t_k-\tau)^{1-\alpha}}. \quad (16)$$

Using again the theorem on additivity of an integral with respect to the integration interval, we get:

$$\begin{aligned}
&\frac{1}{\Gamma(\alpha)}\int_0^{t_k}\frac{1}{(t_k-\tau)^{1-\alpha}}\overline{Q}_\alpha(x,\tau)\,\mathrm{d}\tau \\
&= \frac{1}{\Gamma(\alpha)}\sum_{j=0}^{k-1}\int_{t_j}^{t_{j+1}}\frac{1}{(t_k-\tau)^{1-\alpha}} \\
&\quad\times\left(\overline{Q}_\alpha(x,t_j)\frac{\tau-t_{j+1}}{t_j-t_{j+1}} + \overline{Q}_\alpha(x,t_{j+1})\frac{\tau-t_j}{t_{j+1}-t_j}\right)\mathrm{d}\tau \\
&= \frac{1}{\Gamma(\alpha)}\overline{Q}_\alpha(x,t_0)\int_0^{t_1}\frac{1}{(t_k-\tau)^{1-\alpha}}\frac{\tau-t_1}{t_0-t_1}\,\mathrm{d}\tau \\
&\quad+\frac{1}{\Gamma(\alpha)}\sum_{j=1}^{k-1}\overline{Q}_\alpha(x,t_j)\left(\int_{t_{j-1}}^{t_j}\frac{1}{(t_k-\tau)^{1-\alpha}}\frac{\tau-t_{j-1}}{t_j-t_{j-1}}\,\mathrm{d}\tau\right. \\
&\quad\left.+\int_{t_j}^{t_{j+1}}\frac{1}{(t_k-\tau)^{1-\alpha}}\frac{\tau-t_{j+1}}{t_j-t_{j+1}}\,\mathrm{d}\tau\right) \\
&\quad+\frac{1}{\Gamma(\alpha)}\overline{Q}_\alpha(x,t_k)\int_{t_{k-1}}^{t_k}\frac{1}{(t_k-\tau)^{1-\alpha}}\frac{\tau-t_{k-1}}{t_k-t_{k-1}}\,\mathrm{d}\tau.
\end{aligned}$$

Calculating the following integrals:

$$\begin{aligned}
w_{0,k} &= \frac{1}{\Gamma(\alpha)}\int_0^{t_1}\frac{1}{(t_k-\tau)^{1-\alpha}}\frac{\tau-t_1}{t_0-t_1}\,\mathrm{d}\tau \\
&= \frac{(\Delta t)^\alpha}{\Gamma(2+\alpha)}\left((\alpha+1-k)k^\alpha + (k-1)^{\alpha+1}\right), \quad (17)
\end{aligned}$$

$$\begin{aligned}
w_{j,k} &= \frac{1}{\Gamma(\alpha)}\left(\int_{t_{j-1}}^{t_j}\frac{1}{(t_k-\tau)^{1-\alpha}}\frac{\tau-t_{j-1}}{t_j-t_{j-1}}\,\mathrm{d}\tau\right. \\
&\quad\left.+\int_{t_j}^{t_{j+1}}\frac{1}{(t_k-\tau)^{1-\alpha}}\frac{\tau-t_{j+1}}{t_j-t_{j+1}}\,\mathrm{d}\tau\right) \\
&= \frac{(\Delta t)^\alpha}{\Gamma(2+\alpha)}\left((k-j+1)^{\alpha+1}\right. \\
&\quad\left.-2(k-j)^{\alpha+1}+(k-j-1)^{\alpha+1}\right), \quad (18)
\end{aligned}$$

$$\begin{aligned}
w_{k,k} &= \frac{1}{\Gamma(\alpha)}\int_{t_{k-1}}^{t_k}\frac{1}{(t_k-\tau)^{1-\alpha}}\frac{\tau-t_{k-1}}{t_k-t_{k-1}}\,\mathrm{d}\tau \\
&= \frac{(\Delta t)^\alpha}{\Gamma(2+\alpha)}, \quad (19)
\end{aligned}$$

we obtain certain values of the integral kernel of the left-sided Riemann-Liouville integral, determined for the appropriate grid nodes with respect to the time variable t.

Thus, the integral kernel of the left-sided Riemann-Liouville integral can be expressed in the form of weights:

$$w_{j,k} := \frac{(\Delta t)^{\alpha}}{\Gamma(2+\alpha)} \begin{cases} (\alpha+1-k)k^{\alpha} + (k-1)^{\alpha+1}, & j=0, \\ (k-j+1)^{\alpha+1} - 2(k-j)^{\alpha+1} & \\ \quad +(k-j-1)^{\alpha+1}, & 0<j<k, \\ 1, & j=k. \end{cases} \tag{20}$$

To discretize equation (12) with respect to the spatial variable x, the following differential quotient approximates the value of the second-order derivative in mesh node $(i\Delta x, j\Delta t)$:

$$\left(\frac{\partial^2 U(x,t)}{\partial x^2}\right)_{i,j} = \frac{U_{i-1,j} - 2U_{i,j} + U_{i+1,j}}{(\Delta x)^2} + O((\Delta x)^2). \tag{21}$$

Finally, equation (12) in discrete form can be written as:

$$U_{i,k} = U_{i,0} + D_{\alpha} \sum_{j=0}^{k} w_{j,k} \frac{U_{i-1,j} - 2U_{i,j} + U_{i+1,j}}{(\Delta x)^2} + \sum_{j=0}^{k} w_{j,k} Q_{\alpha i,j}, \tag{22}$$

where $U_{i,j}$ and $Q_{i,j}$ denote the approximate values of the functions U and Q at the mesh node $(i\Delta x, j\Delta t)$, respectively.

After some standard mathematical transformations, we get an implicit numerical scheme:

$$-\frac{D_{\alpha} w_{k,k}}{(\Delta x)^2} U_{i-1,k} + \left(1 + \frac{2D_{\alpha} w_{k,k}}{(\Delta x)^2}\right) U_{i,k} - \frac{D_{\alpha} w_{k,k}}{(\Delta x)^2} U_{i+1,k} = U_{i,0} + \sum_{j=0}^{k-1} \frac{D_{\alpha} w_{j,k}}{(\Delta x)^2} \left(U_{i-1,j} - 2U_{i,j} + U_{i+1,j}\right) + \sum_{j=0}^{k} w_{j,k} Q_{\alpha i,j}, \tag{23}$$

which can be written in matrix form

$$\mathbf{A}\mathbf{U}_k = \mathbf{B}, \tag{24}$$

where matrixes $\mathbf{A}$ and $\mathbf{B}$ are defined as

$$\mathbf{A} = \begin{bmatrix} 1+2a & -a & 0 & 0 & \cdots & 0 & 0 & 0 \\ -a & 1+2a & -a & 0 & \cdots & 0 & 0 & 0 \\ 0 & -a & 1+2a & -a & \cdots & 0 & 0 & 0 \\ \vdots & \vdots & \vdots & \vdots & \ddots & \vdots & \vdots & \vdots \\ 0 & 0 & 0 & -a & 1+2a & -a & 0 & 0 \\ \vdots & \vdots & \vdots & \vdots & \ddots & \vdots & \vdots & \vdots \\ 0 & 0 & 0 & 0 & \cdots & -a & 1+2a & -a \\ 0 & 0 & 0 & 0 & \cdots & 0 & -a & 1+2a \end{bmatrix},$$

$$\mathbf{B} = \begin{bmatrix} b_1 + aU_{0,k} \\ b_2 \\ b_3 \\ \vdots \\ b_i \\ \vdots \\ b_{m-2} \\ b_{m-1} + aU_{m,k} \end{bmatrix}.$$

The elements of matrixes $\mathbf{A}$ and $\mathbf{B}$ are defined by the formulas:

$$a := \frac{D_{\alpha} w_{k,k}}{(\Delta x)^2},$$

$$b_i := U_{i,0} + \sum_{j=0}^{k-1} D_{\alpha} w_{j,k} \left(U_{i-1,j} - 2U_{i,j} + U_{i+1,j}\right) + \sum_{j=0}^{k} w_{j,k} Q_{\alpha i,j}.$$

4. NUMERICAL EXAMPLES

In order to validate the developed numerical method, three examples of initial-boundary value problems are presented for which closed analytical solutions are known. Sixty-four simulations were run for each of the examples. The following parameters values were adopted:

i) the generalized diffusion coefficient $D_{\alpha} = 1$,
ii) the order of the left-sided Caputo derivative $\alpha \in \{0.25, 0.5, 0.75, 0.9999\}$,
iii) the mesh parameters: $L = 1$, $T = 1$, $(\Delta x, \Delta t) \in \left\{\frac{1}{25}, \frac{1}{50}, \frac{1}{100}, \frac{1}{200}\right\} \times \left\{\frac{1}{25}, \frac{1}{50}, \frac{1}{100}, \frac{1}{200}\right\}$.

4.1. Example 1

Consider the first subdiffusion equation with a nonlinear source term

$${}^{C}D^{\alpha}_{0+,t} U(x,t) = \frac{\partial^2 U(x,t)}{\partial x^2} + \frac{1}{6}\left(\frac{(x+1)(2x-3)t^{2-\alpha}}{\Gamma(3-\alpha)} - 2t^2 + 8\right), \tag{25}$$

supplemented with the boundary conditions

$$U(0,t) = -\frac{1}{4}(t-2)(t+2), \tag{26}$$

$$U(1,t) = -\frac{1}{6}(t-2)(t+2), \tag{27}$$

and initial condition

$$U(x,0) = -\frac{1}{3}(x+1)(2x-3). \tag{28}$$

The solution to the initial-boundary value problem (IBVP) given by equations (25)–(28) can be expressed by the function of two variables defined by the formula:

$$U(x,t) = \frac{1}{12}(t-2)(t+2)(x+1)(2x-3), \tag{29}$$

the approximation of which is shown in Fig. 1.

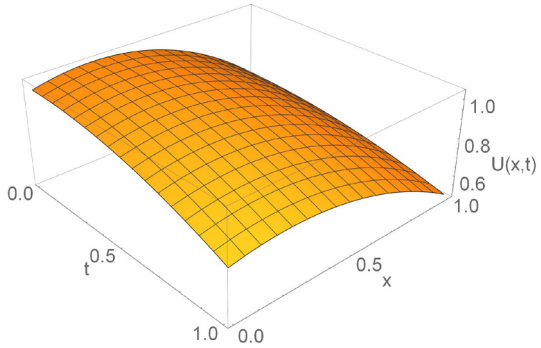

Fig. 1. The numerical solution of the initial-boundary value problem from the first example for $\alpha = 0.9999$

Figures 2–5 show the absolute error generated by the proposed numerical method depending on the order of the Caputo derivative. All the presented figures have a common feature as they show the smallest error value close to the boundary conditions, i.e., for $x = 0$, $x = 1$ and its largest value near the initial condition, i.e., for $t = 0$.

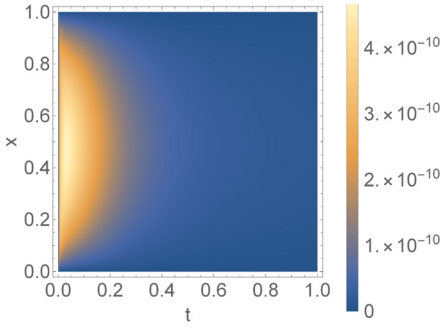

Fig. 2. The absolute error generated by the numerical method for the first example, $\alpha = 0.9999$, $\Delta x = \frac{1}{200}$, $\Delta t = \frac{1}{200}$

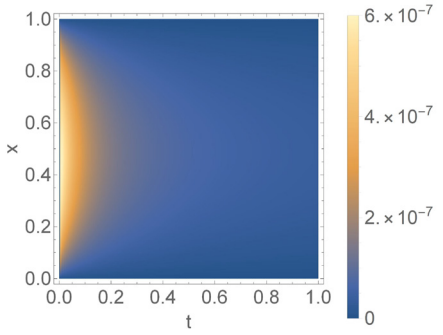

Fig. 3. The absolute error generated by the numerical method for the first example, $\alpha = 0.75$, $\Delta x = \frac{1}{200}$, $\Delta t = \frac{1}{200}$

Tables 1–4 show the mean absolute errors generated by the numerical method in the $[0, 1] \times [0, 1]$ area for sixteen mesh variants and four values of the order of the Caputo derivative. Among all the results, those presented in Table 1 deserve special attention, as they indicate that the scheme works most accurately for $\alpha = 0.9999$. Moreover, all four tables confirm a certain dependence such us a two-fold reduction of the mesh time step results in a nearly four-fold reduction in the mean absolute error.

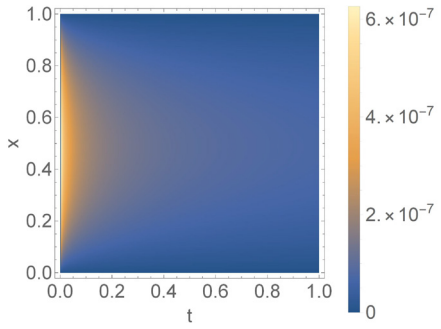

Fig. 4. The absolute error generated by the numerical method for the first example, $\alpha = 0.5$, $\Delta x = \frac{1}{200}$, $\Delta t = \frac{1}{200}$

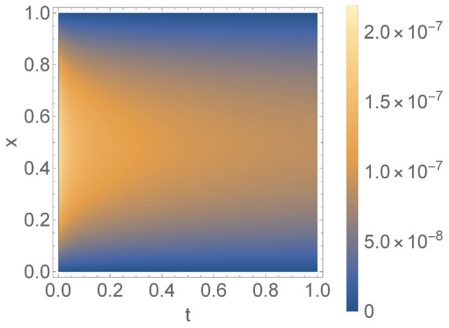

Fig. 5. The absolute error generated by the numerical method for the first example, $\alpha = 0.25$, $\Delta x = \frac{1}{200}$, $\Delta t = \frac{1}{200}$

Table 1
The average absolute error generated by the numerical method for the first example, $\alpha = 0.9999$

	$m = 25$	$m = 50$	$m = 100$	$m = 200$
$n = 25$	3.03e-9	3.093e-9	3.124e-9	3.14e-9
$n = 50$	8.585e-10	8.762e-10	8.852e-10	8.896e-10
$n = 100$	2.387e-10	2.436e-10	2.461e-10	2.473e-10
$n = 200$	6.549e-11	6.685e-11	6.753e-11	6.787e-11

Table 2
The average absolute error generated by the numerical method for the first example, $\alpha = 0.75$

	$m = 25$	$m = 50$	$m = 100$	$m = 200$
$n = 25$	4.077e-6	4.162e-6	4.204e-6	4.226e-6
$n = 50$	1.083e-6	1.105e-6	1.116e-6	1.122e-6
$n = 100$	2.827e-7	2.886e-7	2.915e-7	2.93e-7
$n = 200$	7.304e-8	7.456e-8	7.532e-8	7.57e-8

Table 3
The average absolute error generated by the numerical method for the first example, $\alpha = 0.5$

	$m = 25$	$m = 50$	$m = 100$	$m = 200$
$n = 25$	4.75e-6	4.849e-6	4.898e-6	4.923e-6
$n = 50$	1.236e-6	1.262e-6	1.275e-6	1.281e-6
$n = 100$	3.169e-7	3.235e-7	3.268e-7	3.284e-7
$n = 200$	8.053e-8	8.22e-8	8.304e-8	8.346e-8

Table 4
The average absolute error generated by the numerical method for the first example, $\alpha = 0.25$

	$m = 25$	$m = 50$	$m = 100$	$m = 200$
$n = 25$	3.735e-6	3.812e-6	3.851e-6	3.871e-6
$n = 50$	9.956e-7	1.016e-6	1.027e-6	1.032e-6
$n = 100$	2.61e-7	2.664e-7	2.692e-7	2.705e-7
$n = 200$	6.767e-8	6.908e-8	6.978e-8	7.013e-8

4.2. Example 2

Consider the second subdiffusion equation with a nonlinear source term

$$ {}^{C}D^{\alpha}_{0+,t}U(x,t) = \frac{\partial^2 U(x,t)}{\partial x^2} + t^2 - 16e^{-(x-1)^4}(x-1)^6 + 12e^{-(x-1)^4}(x-1)^2, \quad (30) $$

supplemented with the boundary conditions

$$ U(0,t) = \frac{1}{e} - \frac{2\sin(\pi\alpha)\Gamma(-\alpha-2)t^{\alpha+2}}{\pi}, \quad (31) $$

$$ U(1,t) = 1 - \frac{2\sin(\pi\alpha)\Gamma(-\alpha-2)t^{\alpha+2}}{\pi}, \quad (32) $$

and initial condition

$$ U(x,0) = e^{-(x-1)^4}. \quad (33) $$

The solution to the initial-boundary value problem given by equations (30)–(33) can be expressed by the function of two variables defined by the formula:

$$ U(x,t) = e^{-(x-1)^4} - \frac{2\sin(\pi\alpha)\Gamma(-\alpha-2)t^{\alpha+2}}{\pi}. \quad (34) $$

the approximation of which is shown in Fig. 6.

The distribution of absolute errors presented in Figs. 7–10 clearly shows that its least values occur near the boundary conditions, i.e., for $x = 0$, $x = 1$ and its largest value near the $x = 0.3$.

The analysis of the results collected in Tables 5–8 shows that a simultaneous double reduction of the time and spatial steps (elements on the diagonal) increases the accuracy of the numerical scheme about four times.

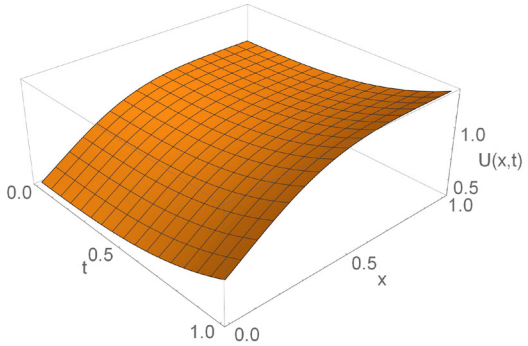

Fig. 6. The numerical solution of the initial-boundary value problem from the second example for $\alpha = 0.9999$

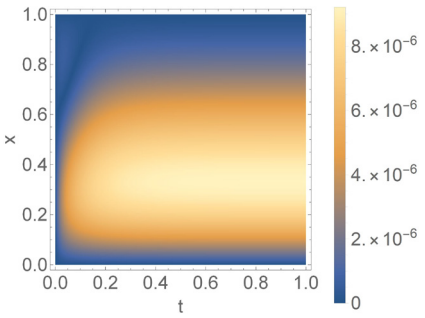

Fig. 7. The absolute error generated by the numerical method for the second example, $\alpha = 0.9999$, $\Delta x = \frac{1}{200}$, $\Delta t = \frac{1}{200}$

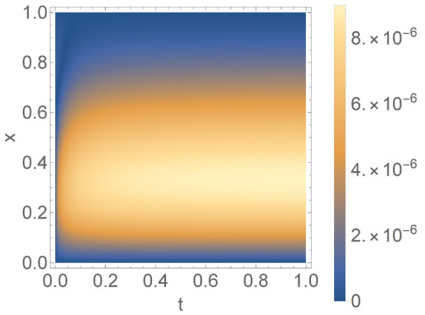

Fig. 8. The absolute error generated by the numerical method for the second example, $\alpha = 0.75$, $\Delta x = \frac{1}{200}$, $\Delta t = \frac{1}{200}$

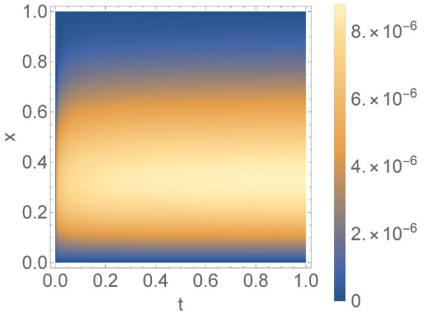

Fig. 9. The absolute error generated by the numerical method for the second example, $\alpha = 0.5$, $\Delta x = \frac{1}{200}$, $\Delta t = \frac{1}{200}$

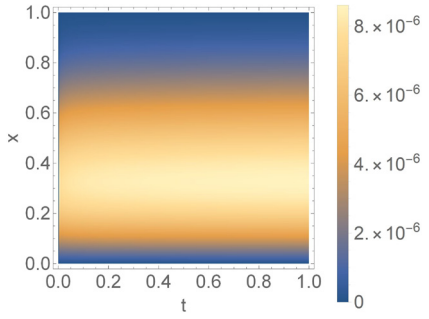

Fig. 10. The absolute error generated by the numerical method for the second example, $\alpha = 0.25$, $\Delta x = \frac{1}{200}$, $\Delta t = \frac{1}{200}$

Table 5
The average absolute error generated by the numerical method for the second example, $\alpha = 0.9999$

	$m = 25$	$m = 50$	$m = 100$	$m = 200$
$n = 25$	2.701e-4	8.313e-5	3.556e-5	2.36e-5
$n = 50$	2.584e-4	6.942e-5	2.117e-5	9.011e-6
$n = 100$	2.56e-4	6.612e-5	1.76e-5	5.341e-6
$n = 200$	2.557e-4	6.537e-5	1.673e-5	4.432e-6

Table 6
The average absolute error generated by the numerical method for the second example, $\alpha = 0.75$

	$m = 25$	$m = 50$	$m = 100$	$m = 200$
$n = 25$	2.678e-4	8.244e-5	3.521e-5	2.332e-5
$n = 50$	2.562e-4	6.887e-5	2.102e-5	8.941e-6
$n = 100$	2.538e-4	6.558e-5	1.747e-5	5.306e-6
$n = 200$	2.535e-4	6.483e-5	1.659e-5	4.399e-6

Table 7
The average absolute error generated by the numerical method for the second example, $\alpha = 0.5$

	$m = 25$	$m = 50$	$m = 100$	$m = 200$
$n = 25$	2.666e-4	8.155e-5	3.434e-5	2.245e-5
$n = 50$	2.559e-4	6.868e-5	2.086e-5	8.787e-6
$n = 100$	2.537e-4	6.553e-5	1.744e-5	5.281e-6
$n = 200$	2.535e-4	6.481e-5	1.659e-5	4.394e-6

Table 8
The average absolute error generated by the numerical method for the second example, $\alpha = 0.25$

	$m = 25$	$m = 50$	$m = 100$	$m = 200$
$n = 25$	2.631e-4	7.783e-5	3.055e-5	1.863e-5
$n = 50$	2.558e-4	6.806e-5	2.008e-5	7.959e-6
$n = 100$	2.546e-4	6.562e-5	1.733e-5	5.116e-6
$n = 200$	2.546e-4	6.507e-5	1.662e-5	4.375e-6

4.3. Example 3

Consider the third subdiffusion equation with a nonlinear source term

$$
\begin{aligned}
{}^{C}D^{\alpha}_{0+,t}U(x,t) &= \frac{\partial^2 U(x,t)}{\partial x^2} \\
&+ \pi^{3/2}2^{\alpha-4}(x+1)(2x-3)t_1^{2-\alpha}\widetilde{F}_2\left(1;\frac{3}{2}-\frac{\alpha}{2},2-\frac{\alpha}{2};-\frac{1}{16}\pi^2t^2\right) \\
&+ \frac{4\cos\left(\frac{\pi t}{2}\right)}{\pi},
\end{aligned}
\tag{35}
$$

supplemented with the boundary conditions

$$
U(0,t) = \frac{3\cos\left(\frac{\pi t}{2}\right)}{\pi}, \tag{36}
$$

$$
U(1,t) = \frac{2\cos\left(\frac{\pi t}{2}\right)}{\pi}, \tag{37}
$$

and initial condition

$$
U(x,0) = -\frac{(x+1)(2x-3)}{\pi}. \tag{38}
$$

The solution to the initial-boundary value problem given by equations (35)–(38) can be expressed by the function of two variables defined by the formula:

$$
U(x,t) = -\frac{(x+1)(2x-3)\cos\left(\frac{\pi t}{2}\right)}{\pi}. \tag{39}
$$

Figure 11 shows the approximate solution of the IBVP from the third example obtained for $\alpha = 0.9999$, $\Delta x = \frac{1}{200}$, $\Delta t = \frac{1}{200}$.

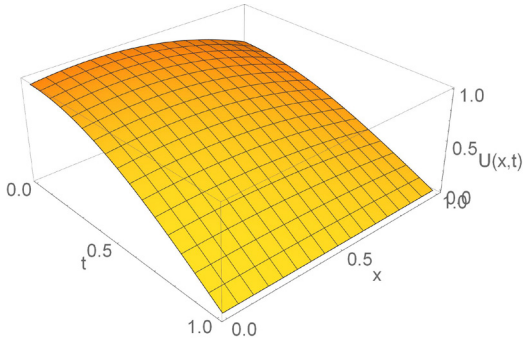

Fig. 11. The numerical solution of the initial-boundary value problem from the third example for $\alpha = 0.9999$

Figures 12–15 show the very interesting behavior of the absolute error generated by the numerical method. In all cases, its lowest value is observed in the vicinity of the boundary conditions, i.e., for $x = 0$, $x = 1$. In the case of $\alpha = 0.9999$, its highest value is observed for a large t. Decreasing the value of the order of the Caputo derivative results in the scheme beginning to generate the greatest errors for a small t.

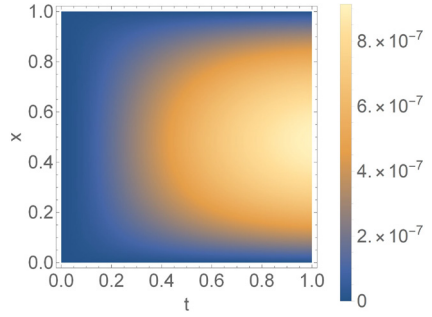

Fig. 12. The absolute error generated by the numerical method for the third example, $\alpha = 0.9999$, $\Delta x = \frac{1}{200}$, $\Delta t = \frac{1}{200}$

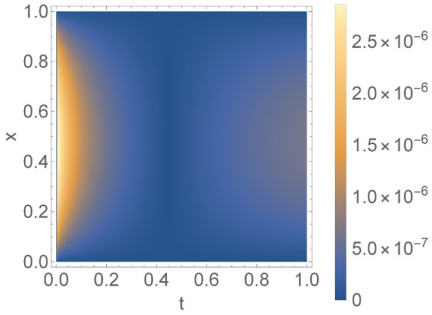

Fig. 13. The absolute error generated by the numerical method for the third example, $\alpha = 0.75$, $\Delta x = \frac{1}{200}$, $\Delta t = \frac{1}{200}$

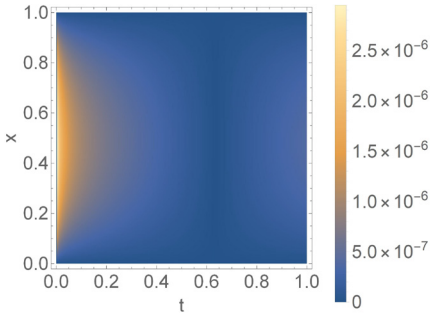

Fig. 14. The absolute error generated by the numerical method for the third example, $\alpha = 0.5$, $\Delta x = \frac{1}{200}$, $\Delta t = \frac{1}{200}$

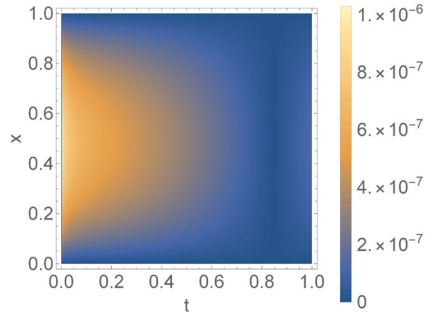

Fig. 15. The absolute error generated by the numerical method for the third example, $\alpha = 0.25$, $\Delta x = \frac{1}{200}$, $\Delta t = \frac{1}{200}$

Based on the results collected in Tables 9–12, we can draw similar conclusions as in the case of the first example like a two-fold reduction of the mesh time step results in a nearly four-fold reduction in the mean absolute error.

Table 9
The average absolute error generated by the numerical method for the third example, $\alpha = 0.9999$

	$m = 25$	$m = 50$	$m = 100$	$m = 200$
$n = 25$	2.048e-5	2.09e-5	2.112e-5	2.122e-5
$n = 50$	5.127e-6	5.234e-6	5.288e-6	5.315e-6
$n = 100$	1.283e-6	1.31e-6	1.323e-6	1.33e-6
$n = 200$	3.209e-7	3.276e-7	3.309e-7	3.326e-7

Table 10
The average absolute error generated by the numerical method for the third example, $\alpha = 0.75$

	$m = 25$	$m = 50$	$m = 100$	$m = 200$
$n = 25$	1.968e-5	2.009e-5	2.029e-5	2.04e-5
$n = 50$	5.173e-6	5.281e-6	5.335e-6	5.362e-6
$n = 100$	1.344e-6	1.372e-6	1.386e-6	1.393e-6
$n = 200$	3.461e-7	3.533e-7	3.569e-7	3.587e-7

Table 11
The average absolute error generated by the numerical method for the third example, $\alpha = 0.5$

	$m = 25$	$m = 50$	$m = 100$	$m = 200$
$n = 25$	1.585e-5	1.618e-5	1.634e-5	1.642e-5
$n = 50$	4.154e-6	4.24e-6	4.283e-6	4.305e-6
$n = 100$	1.071e-6	1.094e-6	1.105e-6	1.11e-6
$n = 200$	2.735e-7	2.792e-7	2.82e-7	2.834e-7

Table 12
The average absolute error generated by the numerical method for the third example, $\alpha = 0.25$

	$m = 25$	$m = 50$	$m = 100$	$m = 200$
$n = 25$	1.082e-5	1.105e-5	1.116e-5	1.122e-5
$n = 50$	2.901e-6	2.962e-6	2.992e-6	3.007e-6
$n = 100$	7.629e-7	7.788e-7	7.867e-7	7.907e-7
$n = 200$	1.981e-7	2.023e-7	2.043e-7	2.054e-7

5. DISCUSSION

Anomalous subdiffusion is a physical process whose existence is confirmed by experimental research. They are solved analytically, but only in some specific cases. The computational examples presented in the fourth chapter were to confirm the correct

operation of the proposed numerical method. Analytical solutions used for method validation were obtained by solving the initial-boundary value problems "from the end" - first a solution was established, and then the appropriate boundary conditions, initial condition and source term were adjusted. This procedure allows to obtain simple analytical solutions with the source term which can only be considered theoretically – it loses the physical aspect.

The proposed approach, however, has a certain limitation, it does not solve the problems with source term of the form $Q_\alpha(x,t,U(x,t))$, which is typical for the reaction-diffusion equation. The further work plan assumes the improvement of the proposed method of solving the subdiffusion equation with the source term dependent on the function U.

6. CONCLUSIONS

The method proposed in the paper is an extension of the generalized Crank-Nicolson method for the one-dimensional subdiffusion equation, where the source term is additionally taken into account. In the part of the method where the left-sided Riemann-Liouville integral was discretized, minor changes were made in the nodes numbering, which resulted in a more concise notation. The obtained numerical results are largely consistent with closed analytical solutions. The numerous simulations that were carried out for the three examples (192 in total) did not indicate that the method was unstable in any of them. On the basis of the obtained results, it can also be concluded that the method is convergent. Let us point out that the method can be extended to the multidimensional case.

7. NOMENCLATURE

x	– space variable
t	– time variable
L	– fixed value of x
T	– fixed value of t
Δx	– space step size
Δt	– time step size
Π	– considered region
i,j,k,m,n	– natural numbers
w	– discrete form of the integral kernel of the left-sided Riemann-Liouville integral
$\mathbf{A}$	– matrix
$\mathbf{B}$	– vector
$\mathbf{U_k}$	– vector
U	– concentration
Q_α	– source term
${}_pF_q$	– generalized hypergeometric function
${}_p\tilde{F}_q$	– regularized generalized hypergeometric function
D	– diffusion coefficient
D_α	– generalized diffusion coefficient
I^α_{0+}	– left-sided Riemann-Liouville integral
${}^CD^\alpha_{0+}$	– left-sided Caputo derivative
α	– fractional order

REFERENCES

[1] T. Kosztołowicz, K. Dworecki, and S. Mrówczyński, "How to measure subdiffusion parameters," *Phys. Rev. Lett.*, vol. 94, p. 170602, 2005, doi: 10.1016/j.tins.2004.10.007.

[2] T. Kosztołowicz, K. Dworecki, and S. Mrówczyński, "Measuring subdiffusion parameters," *Phys. Rev. E*, vol. 71, p. 041105, 2005.

[3] E. Weeks, J. Urbach, and L. Swinney, "Anomalous diffusion in asymmetric random walks with a quasi-geostrophic flow example," *Physica D*, vol. 97, pp. 291–310, 1996.

[4] T. Solomon, E. Weeks, and H. Swinney, "Observations of anomalous diffusion and Lévy flights in a 2-dimensional rotating flow," *Phys. Rev. Lett.*, vol. 71, pp. 3975–3979, 1993.

[5] N.E. Humphries, *et al.*, "Environmental context explains Lévy and Brownian movement patterns of marine predators," *Nature*, vol. 465, pp. 1066–1069, 2010.

[6] U. Siedlecka, "Heat conduction in a finite medium using the fractional single-phase-lag model," *Bull. Pol. Acad. Sci. Tech. Sci.*, vol. 67, pp. 402–407, 2019.

[7] R. Metzler and J. Klafter, "The random walk:s guide to anomalous diffusion: a fractional dynamics approach," *Phys. Rep.*, vol. 339, pp. 1–77, 2000.

[8] R. Metzler and J. Klafter, "The restaurant at the end of the random walk: recent developments in the description of anomalous transport by fractional dynamics," *J. Phys. A: Math. Gen.*, vol. 37, pp. 161–208, 2004.

[9] M. Aslefallah, S. Abbasbandy, and E. Shivanian, "Numerical solution of a modified anomalous diffusion equation with nonlinear source term through meshless singular boundary method," *Eng. Anal. Boundary Elem.*, vol. 107, pp. 198–207, 2019.

[10] Y. Li and D. Wang, "Improved efficient difference method for the modified anomalous sub-diffusion equation with a nonlinear source term," *Int. J. Comput. Math.*, vol. 94, pp. 821–840, 2017.

[11] X. Cao, X. Cao, and L. Wen, "The implicit midpoint method for the modified anomalous sub-diffusion equation with a nonlinear source term," *J. Comput. Appl. Math.*, vol. 318, pp. 199–210, 2017.

[12] A. Kilbas, H. Srivastava, and J. Trujillo, *Theory and Applications of Fractional Differential Equations*. Amsterdam: Elsevier, 2006.

[13] E.D. Rainville, *Special Functions*. New York: The Macmillan Company, 1960.

[14] J.-L. Liu and H.MSrivastava, "Classes of meromorphically multivalent functions associated with the generalized hypergeometric function," *Math. Comput. Modell.*, vol. 39, pp. 21–34, 2004.

[15] Y.L. Luke, "Inequalities for generalized hypergeometric functions," *J. Approximation Theory*, vol. 5, pp. 41–65, 1972.

[16] M. Włodarczyk and A. Zawadzki, "The application of hypergeometric functions to computing fractional order derivatives of sinusoidal functions," *Bull. Pol. Acad. Sci. Tech. Sci.*, vol. 64, pp. 243–248, 2016.

[17] M. Błasik, "A generalized Crank-Nicolson method for the solution of the subdiffusion equation," *23rd International Conference on Methods & Models in Automation & Robotics (MMAR)*, pp. 726–729, 2018.

[18] M. Błasik, "Zagadnienie stefana niecałkowitego rzędu," Ph.D. dissertation, Politechnika Częstochowska, 2013.

[19] M. Błasik and M. Klimek, "Numerical solution of the one phase 1d fractional stefan problem using the front fixing method," *Math. Methods Appl. Sci.*, vol. 38, no. 15, pp. 3214–3228, 2015.

[20] K. Diethelm, *The Analysis of Fractional Differential Equations*. Berlin: Springer-Verlag, 2010.